



TC4 Newsletter Vol. 13, November, 2013

Inside this Issue

Article 1: Workshop Report: Whole Atmospheric Coupling during solar cycle 24.....	1
Article 2: Resolute FPI for Polar Cap thermospheric and mesospheric wind observation.....	2
Article 3: Analysis of atmospheric coupling in actual events using a whole atmosphere-ionosphere model.....	4
Article 4: Ionospheric Delay Gradient Experiments at the vicinity of Suvarnabhumi International Airport, Bangkok, Thailand.....	5
Article 5: On the application of FPI for thermospheric wind observation: day and night...	6
Article 6: Concentric waves and short-period oscillations observed in the ionosphere after 2013 Moore EF5 tornado.....	9
Meeting list and "From the Editor".....	11

Article 1

Workshop Report: Whole Atmospheric Coupling during Solar Cycle 24 National Central University, Jhongli, Taiwan, July 14-17, 2013

Loren C. Chang¹, Nanan Balan¹, Mao-Chang Liang², Jann-Yenq Liu¹, Chien-Hung Lin³

1. Institute of Space Science, National Central University, Taiwan; 2. Research Center for Environmental Changes, Academia Sinica, Taiwan; 3. Department of Earth Sciences, National Cheng Kung University, Taiwan.



Loren C. Chang

Since the start of Solar Cycle 24 in 2008, there has been an explosion of scientific results highlighting the importance of vertical coupling between all layers of the atmosphere, as well as between the atmosphere as a whole and the Sun. From upper atmospheric and ionospheric variability driven by atmospheric waves and tides excited by tropical rainfall in the troposphere, to potential signatures of magnetosphere and solar sources

in the lower atmosphere, it is apparent that a system-wide approach incorporating scientists from all atmospheric regions is necessary to tackle the new challenges of both space and atmospheric weather and climate.

To help build new lines of communication between these different communities in CAWSES-II activities,



Figure 1: WATM24 participants who made it past Typhoon Soulik on day 1.

and review recent advances affecting TG4, the Workshop on Whole Atmospheric Coupling during Solar Cycle 24 (WATM24) was held at National Central University (NCU) in Jhongli, Taiwan from July 14 – 17, 2013. Financial support was kindly provided by the Taiwan National Science Council and TG4, while facilities and additional support were provided by NCU and the students and staff of NCU. As a reminder on the importance of atmospheric variability, Taiwan was hit by Typhoon Soulik on July 12 and 13, causing flight delays and several fallen branches around the NCU campus. For attendees who arrived early, the typhoon provided the experience of seeing what 50 m s^{-1} winds look like at the bottom of the atmospheric column!

Despite the typhoon, attendance was strong with a total of 55 registered scientists and students, including 18 international attendees from institutions in the USA, Bulgaria, India, and Japan. 38 oral presentations were given, including both invited reports on new advances, as well as longer tutorial-style reviews of subjects pertaining to the CAWSES-II activities. Major themes covered throughout the four days of the workshop included tides in the thermosphere and ionosphere, ionosphere-thermosphere coupling, tropical rainfall variability responsible for tidal and wave excitation, downwards coupling between the stratosphere and troposphere, gravity wave-driven middle atmospheric oscillations, the global electric circuit, lithosphere-atmosphere coupling, severe space weather events driven by intense CMEs (coronal mass ejections), as well as middle and lower atmospheric changes driven by solar and anthropogenic sources. The talks were accompanied by enthusiastic discussions, as well as questions from students and scientists.



Figure 2. Professor Kazuo Shiokawa (Nagoya U., Japan) leads a discussion on atmosphere-ionosphere coupling over lunch.

Dedicated discussion sessions were also held over lunch, as well as on the final afternoon of the workshop, where participants discussed future prospects for CAWSES-II science. Topics and proposals discussed included encouraging the development of constellations of small satellites as both educational and scientific platforms, prediction of severe space weather events, the need to engage with the tropospheric community, as well as questions concerning atmospheric coupling with the solid Earth and cryosphere. The workshop then adjourned as planned, just in time for Typhoon Cimaron to sweep by. Overall, the workshop was a success with new connections being made, while laying the groundwork for future collaborations. An archive of presentations is being compiled, and is available at: <http://www.ss.ncu.edu.tw/~wadm24/schedule.html>

Article 2

Resolute Fabry-Perot Interferometer for Polar Cap Thermospheric and Mesospheric Wind Observations

Qian Wu

National Center for Atmospheric Research. Boulder, Co USA.



Qian Wu

Resolute, Canada (75N, 93W, MLAT 83N) is the home of the Advanced Modular Incoherent Scatter Radar (AMISR) the phased array incoherent scatter radar. Before the installation of AMISR, a Fabry Perot interferometer (FPI) for thermospheric and mesospheric wind observation was deployed at Resolute with the US National Science Foundation support in 2002.

One objective of the FPI deployment is to study the ion neutral interaction inside the polar cap, which has a great importance to understand how the energy from the magnetosphere is transferred to the ionosphere and ther-

mosphere. Polar cap is the source region of the space weather related to geomagnetic substorms. Ion-neutral interaction leads to joule heating. Knowing thermospheric winds can lead to a more accurate estimation of the joule heating. Joule heating can cause up welling in the thermosphere and altering the composition causing heavier molecules move to higher altitude. Consequently, ion production and loss balance changes and reduces the ion density. Joule heating also changes the thermospheric dynamics and the neutral winds, which can carry the ion depleted ionosphere to mid latitudes causing negative storm effect. Hence the thermospheric winds are a key parameter for understanding how the iono-



sphere responds to a substorm.

Another objective is to study the mesospheric and lower thermospheric dynamics inside the polar cap, where both migrating and nonmigrating tides are significant. Also in the polar cap, the vertical coupling from the stratosphere to mesosphere and possibly to the thermosphere take place during sudden stratospheric warming events (SSW). Recent observations have suggested that SSW can impact the ionosphere even in mid and low

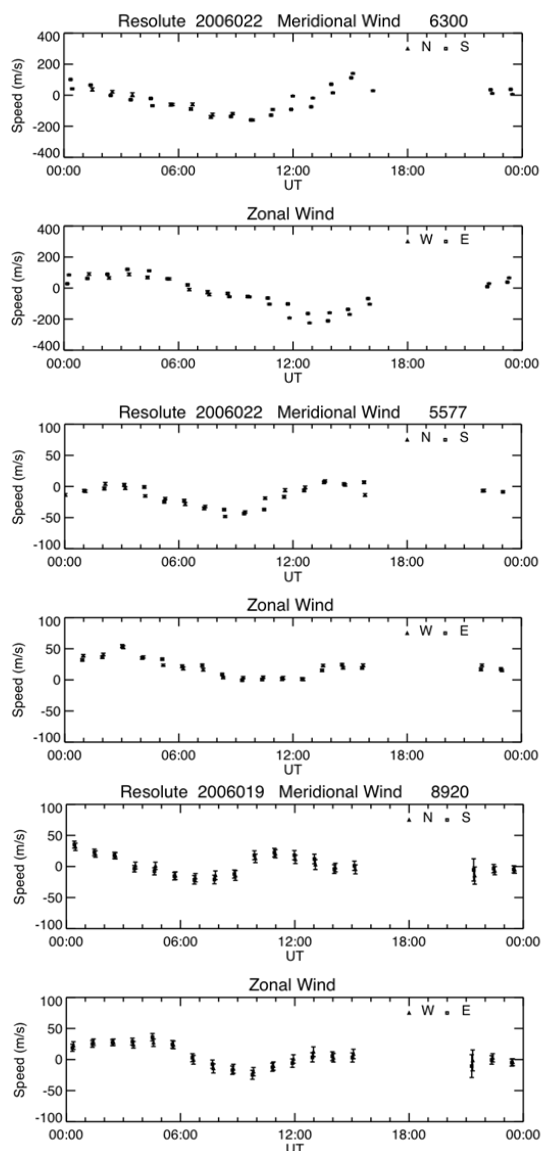


Figure 1. Mesospheric and thermospheric winds measured by Resolute FPI. Thermospheric winds from the O 630 nm emission (~ 250 km) showed mostly diurnal variation, which is a reflection of the mostly antisunward winds. The local midnight is 6 UT and noon at 18 UT. The data gap near 18 UT is due to daylight condition. Both the lower thermospheric winds (O 557.7 nm at 97 km) and mesospheric winds (OH 892 nm at 87 km) showed strong semidiurnal tides. At this latitude (75N) both migrating and nonmigrating tides contribute to the overall wind field.

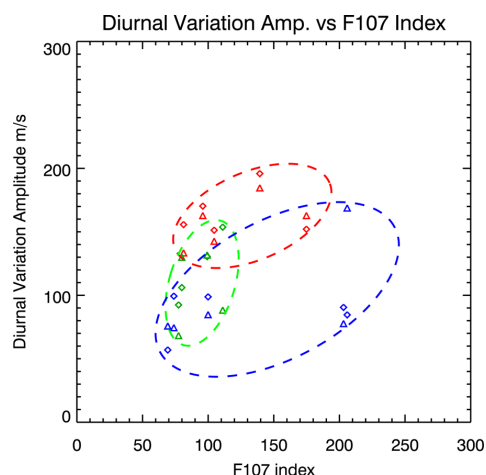


Figure 2. Polar cap thermospheric wind diurnal variations (antisunward wind speed) vs solar F10.7 index at Resolute (green), Eureka (red), Thule (blue). Consistent larger winds were observed at Eureka [Wu et al. 2008, JASTP 70, p2014-2030]. That seems to suggest that there are more thermospheric wind structures inside the polar cap than we had expected. Plan for simultaneous observations at the three stations are under consideration to further explore the thermospheric dynamics in the polar cap.

latitudes. Ionospheric effect of the SSW is a focus of many recent studies.

To achieve these objectives, the Resolute FPI is designed to measure nighttime thermospheric and mesospheric winds with multi-emission capability. There are three filters in the FPI for the O 630 nm (~ 250km), O 557.7 nm (~ 97 km), and OH 892 nm (~ 87 km) airglow emissions. The instrument measures winds by recording the Doppler shift in these airglow emissions. The FPI uses a 10 cm clear aperture etalon with 2 cm gap. The integration times are 3 to 5 minutes. The instrument samples four cardinal directions and the zenith. The wind errors are a few meters per second. Examples of the thermospheric and mesospheric winds from the FPI are shown in Figure 1.

The Resolute FPI thermospheric wind data in the 2000s were compared with observations from Thule, Greenland (76N, 69W, MLAT 86) in the 1980s and Eureka, Canada (80N, 86W, MLAT 89) in the 1990s to examine long-term variation inside the polar cap. Large interstation differences were observed as shown in Fig. 2. The thermospheric winds were consistently larger at Eureka and the source for this is unknown. The thermospheric wind inside polar cap may have more complicated structures. Future FPI deployments at Eureka and Thule are under consideration.

The Resolute FPI data are available from the Madrigal database at Millstone Hill observatory at <http://cedar.openmadrigal.org>.



Article 3

Analysis of atmospheric coupling in actual events using a whole atmosphere-ionosphere model

Hidekatsu Jin

National Institute of Information and Communications Technology, Tokyo, Japan



Hidekatsu Jin

I have been participating in a project of model coupling since 2007, when I was a postdoc in NICT. The coupled model is now called GAIA (Ground-to-topside model of Atmosphere and Ionosphere for Aeronomy) [Jin et al., JGR, 2011], which consists of a whole atmospheric model [Miyoshi and Fujiwara, GRL, 2003], an ionospheric model [Shinagawa and Oyama, EPS, 2006], and an electrodynamics model [Jin et al., JGR, 2008], and they have been coupled together self-consistently. As one of the developers of the model, I am interested in making it more realistic so that it can contribute to the prediction of space weather phenomena of both solar and meteorological origins as well as to the better understanding of vertical atmospheric coupling. Comparisons with observations and other models are therefore important for the validation and improvement of the

model as well as for clarifying the physical mechanisms responsible for actual variations in the middle and upper atmosphere.

The following is the results from our recent collaborative study. We compared our model results of the major stratospheric sudden warming in January 2009 with FORMOSAT3/COSMIC and TIMED/SABER observations [Jin et al., JGR, 2012]. The comparison shows general agreement in major features from the stratosphere to the lower thermosphere and ionosphere, including a drastic change in the zonal mean parameters of the polar stratosphere as well as a pronounced semi-diurnal variation in the F region electron density at low latitudes along with its local-time phase shift. The model suggests that the electron density variation is

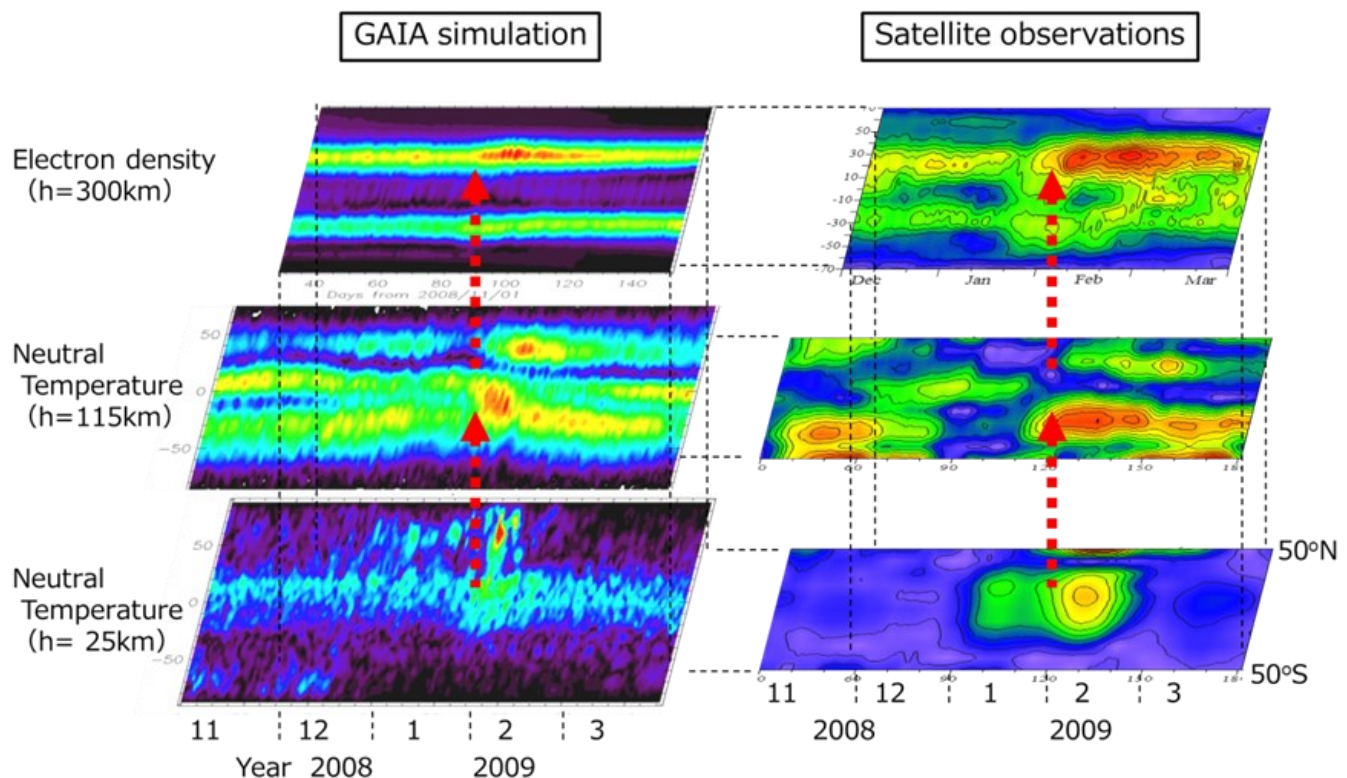


Figure 1. Comparison of the amplitude of SW2 component at different altitudes, extracted from (Left) the GAIA simulation with those from (Right upper) the FORMOSAT-3/COSMIC observation and (Right middle and lower) the TIMED/SABER observation during the period from November 2008 to March 2009. The vertical red arrows indicate the days when an amplification of SW2 tide begins and propagates upward during the initial phase of major stratospheric warming in January 2009 (After Jin et al. [2012]).

caused by an enhanced semidiurnal variation in the $E \times B$ drift, which is related to an amplified semidiurnal migrating tide (SW2) in the lower thermosphere. The changes in the amplitude and phase of SW2 are found at low latitudes from the stratosphere to the lower thermosphere by the model and the TIMED/SABER observation (Figure 1) as well as in the upper thermosphere by a comparison of the model with the GRACE and CHAMP observations (from another study by Liu et al. [GRL, 2013]). We examined a possible mechanism for the SW2 variability in the low latitude stratosphere by analyzing the simulation data set. We found that the low latitude SW2 variability can mostly be accounted for by the variability of first symmetric (2, 2) mode (Figure 2), and that it is caused by the change of its propagation due to the change of zonal mean parameters in the middle atmosphere from its source term analysis.

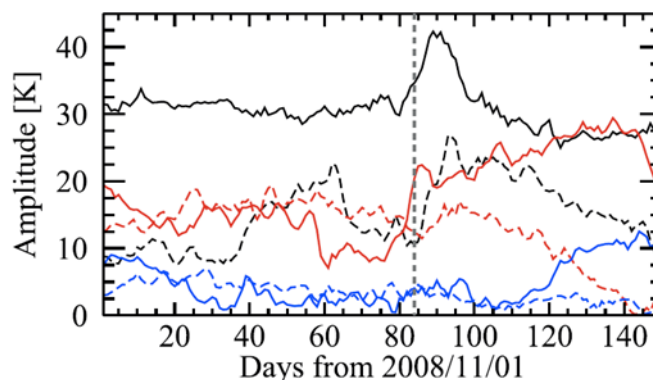


Figure 2. Temporal variations in the amplitude of SW2 Hough modes decomposed from the simulated neutral temperature at 116 km height. The solid curves represent the symmetric modes, (2, 2), (2, 4) and (2, 6) shown in black, red and blue, respectively, while the dashed curves represent the asymmetric modes, (2, 3), (2, 5) and (2, 7) in black, red and blue. The vertical dashed line indicates the day when the criteria for a major SSW are satisfied (Jan 24, 2009) [Jin et al., 2012].

Article 4

Ionospheric Delay Gradient Experiments at the Vicinity of Suvarnabhumi International Airport, Bangkok, Thailand

Pornchai Supnithi¹, Sarawoot Rungraengwajjake¹, Susumu Saito², Nattapong Siansawasdi³

1. Faculty of Engineering, King Mongkut's Institute of Technology Ladkrabang, Bangkok 10520, Thailand, 2. Communication, Navigation and Surveillance Department, Electronic Navigation Research Institute, Tokyo, Japan, 3. Air Navigation Radio Aids Department, Aeronautical Radio of Thailand, Bangkok, Thailand.



Pornchai Supnithi

The global navigation satellite system (GNSS) has become a powerful component for aeronautical navigations. However, the ionospheric delay is still the largest source of errors and degrades the accuracy of GNSS receivers. To improve the accuracy and availability of the system, the differential techniques have been developed to mitigate such error. For aeronautical navigation, the Satellite-Based Augmentation System (SBAS) and Ground-Based Augmentation System (GBAS) have been developed to support all navigation operational levels of the aircrafts. These augmentation systems provide the differential corrections and integrity information to the GNSS receivers that are equipped in the aircrafts. It is now well known that the severe ionospheric disturbances such as the storm-enhanced density (SED) can cause a large ionospheric delay gradient, which affects the availability and integrity requirement of the systems especially for landing approach of GBAS CAT II/III. The current designed GBAS system does

not support very large delay gradient situation. In order to protect the safety level requirements for worldwide operation, therefore, the local ionospheric threat model needs to be developed for all concerned regions. For equatorial and low-latitude regions, particularly, the equatorial anomaly and plasma bubble are common phenomena which can cause the ionospheric delay gradient as well as ionospheric scintillation.

Since 2011, we have implemented the ionospheric delay gradient study for aeronautical applications in anticipation of the solar maximum. This project is supported by the Electronic Navigation Research Institute (ENRI), Japan, Aeronautical Radio of Thailand (Aerothai) as well as partially funded by the National Research Council of Thailand (NRCT). The goal is to investigate the characteristics of the difference of slant Total electron content (dSTEC) in a low-latitude region during the quiet-period (background dSTEC) and the disturbed period

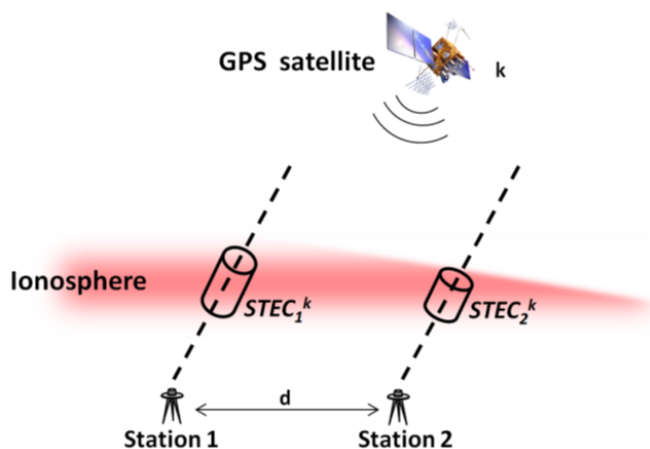


Figure 1. Illustration of ionospheric delay gradient between two monitoring stations.

(related to the plasma bubbles). Figure 1 shows a difference in STEC between two monitoring stations. Three GNSS monitoring stations have been setup near the Suvarnabhumi international airport, Bangkok, Thailand. One is located on the runway of the airport (AERO: 13.6945°N, 100.7608°E). The others are located at King Mongkut's Institute of Technology Ladkrabang (KMIT: 13.7278°N, 100.7726°E) and Stamford International University (STFD: 13.7356°N, 100.6612°E) which are shown in Fig. 2. Two baseline directions can therefore be studied in this work, they are east-west and north-south directions. Figure 3 shows an example of the obtained STEC on the east-west directions during the plasma bubble. The plots show a slight delay of STEC at one station with respect to the other. In addition, the disturbance occurs at around 2100 LT.



Figure 2. Three GPS monitoring stations near Suvarnabhumi airport in this project.

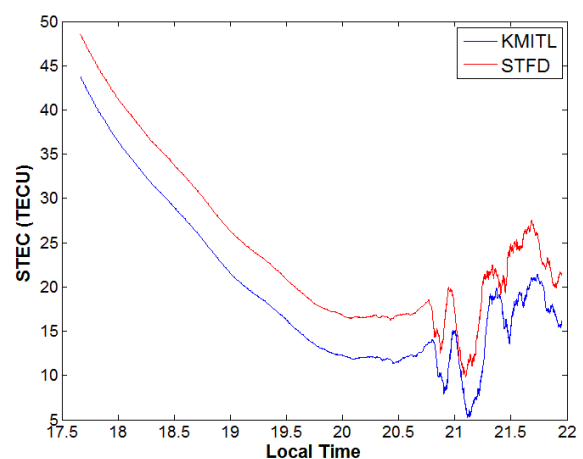


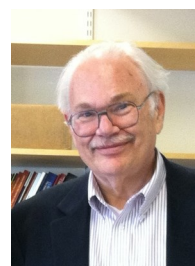
Figure 3. Uncalibrated STEC of PRN5 at KMITL and STFD stations.

Article 5

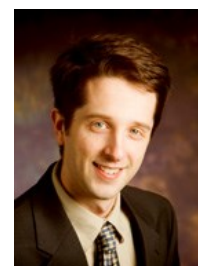
On the application of Fabry-Perot interferometers for thermospheric wind observations: day and night

J. W. Meriwether¹, J. J. Makela², A. J. Gerrard³

1. Department of Physics and Astronomy, Clemson University, Clemson, SC, USA, 2. Department of Electrical and Computer Engineering, University of Illinois at Urbana-Champaign, Urbana, IL, USA, 3. Center for Solar-Terrestrial Research, New Jersey Institute of Technology, Newark, NJ USA.



J. W. Meriwether



J. J. Makela



A. J. Gerrard



As researchers strive to come to a more complete understanding of the global thermosphere-ionosphere (TI) system and the complex coupling and forcings that give rise to extensive day-to-day variability, it has become apparent how important it is to have a broad perspective of geophysical parameters. Across a wide range of mesoscale TI phenomena – such as geomagnetic storm-time dynamics, the characterization of traveling atmos-

pheric disturbances, and studying the solar cycle variability impacts on the climatology of thermosphere dynamics – a detailed study requires extended measurements of the state of both the plasma and neutrals. Knowledge of the direction and magnitude of the vector neutral wind is crucial to the understanding of small-scale dynamical processes such as the development and evolution of ionospheric instabilities (Kudeki et al, 2007), Joule heating in the auroral region (Rees, 1995), and the F-region dynamo at low latitudes (Rishbeth, 1981). However, such observations are sparse because the experimental challenges associated with such measurements are daunting, especially during the daytime. Recently, new capabilities in measuring the neutral winds and temperatures have been developed using robust Fabry-Perot interferometer (FPI) systems capable of being operated over long periods of time with minimal user intervention, opening up the possibility for studying the background neutral winds for all seasons and all phases of the solar cycle.

The FPI makes high spectral resolution measurements of the OI 630-nm atomic emission, which originates through chemical reactions involving the O⁺ ions. The 630-nm airglow layer exists as a broad emission layer in the thermosphere between 200 km and 300 km, peaking in the lower thermosphere at an altitude of ~230 km (Solomon and Abreu, 1989) during the day and at ~250 km at night (Hernandez and Roble, 1995; Meriwether, 2006). The data obtained with this instrument are used to determine the line-of-sight Doppler shift and Doppler broadening for each direction observed, relating to the

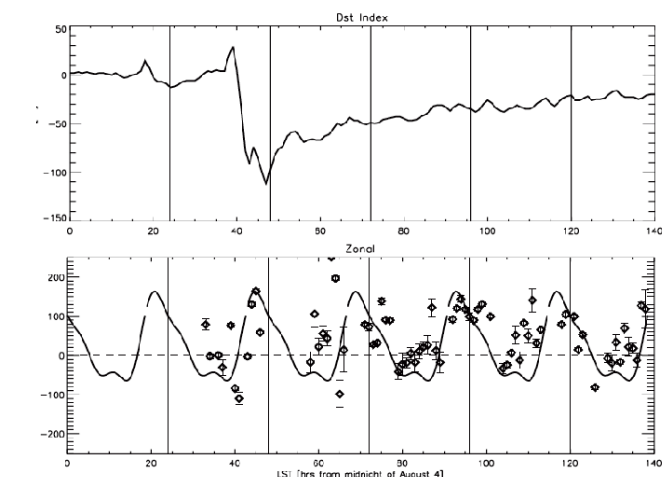


Figure 1. (top) Hourly Dst index for a period in August 2011. Time is measured in LT hours from midnight of August 4. Vertical black lines represent successive days. **(bottom)** Hourly, full diurnal, thermospheric winds as measured by SOFDI from Huancayo, Peru. The black line represents the HWM00 climatology winds. Zonal and meridional winds (not shown) show a high level of afternoon variability (from Earle et al., 2013).

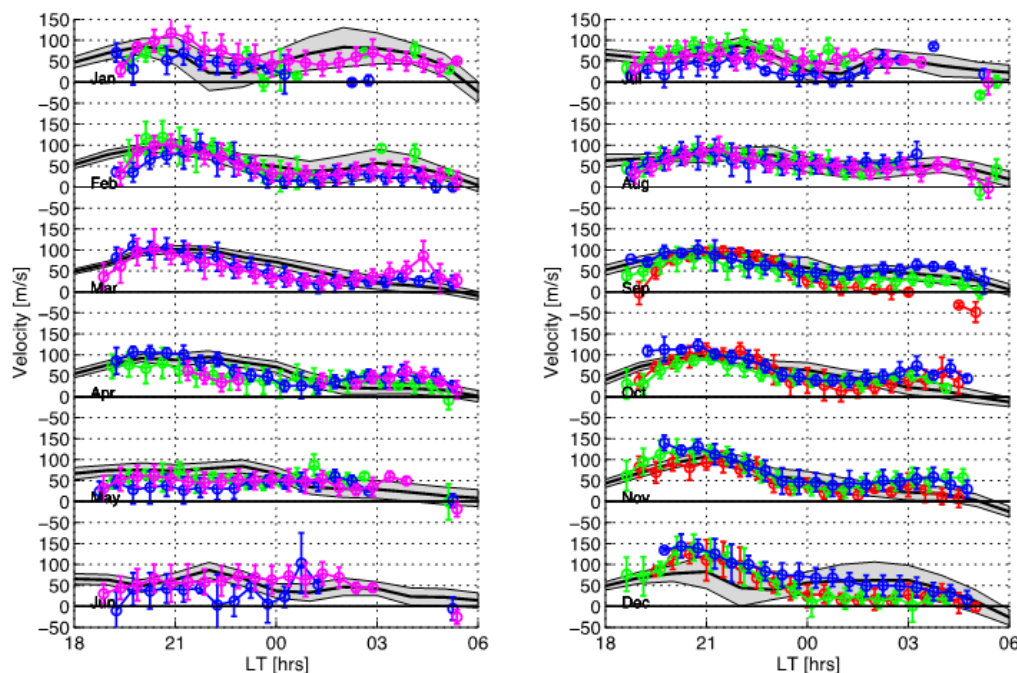


Figure 2. Comparisons of Brazil FPI monthly equatorial zonal wind climatologies for 2009–2012 with WAM monthly model predictions for the solar minimum period. Red lines represent data collected in 2009, green 2010, blue 2011, and pink 2012. The error bars give the standard deviation of the data included in each 30-min bin illustrating the extent of geophysical variability. (from Meriwether et al., 2013)

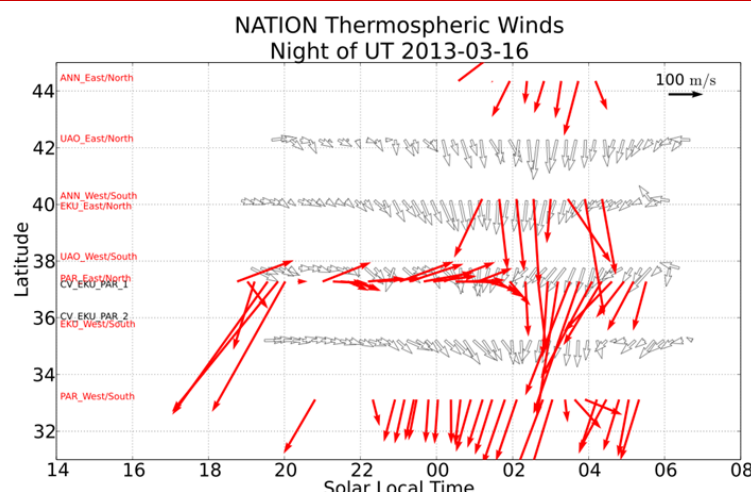


Figure 3. Eastern continental USA thermospheric wind observations (red arrows) for the geomagnetic storm period of March 16, 2013. Also shown for comparison are the white vectors illustrating the monthly-mean winds (from Makela et al., 2013, to be submitted). ANN, UAO, EKV, PAR designate FPI stations located near Ann Arbor, MI, Urbana-Champaign, IL, Richmond, KY, and Brevard, NC, respectively, in the eastern continental United States.

neutral wind and temperature along the line of sight, respectively. The number of such FPI observatories in all regions of the globe has been increasing steadily as the awareness of the importance of such thermospheric data on winds and temperatures has become more highly appreciated. Meriwether (2006) describes the benefits to be achieved by a FPI network, and Makela et al. (2012) present a recent example of a relatively localized example of such a network.

Daytime observations at this wavelength, to date, have been typically limited to emission intensities and are extremely sparse. However, through the application of modern Fabry-Perot technology, as exemplified by the Second-generation Optimized Fabry-Perot Doppler Imager (SOFDI), which uses three Fabry-Perot etalons in series, daytime measurements have been successful yielding continuous 24-hour (i.e., nighttime and daytime) wind and temperature measurements from the upper mesosphere and lower thermosphere (Gerrard and Meriwether, 2012; Earle et al., 2013). This instrument, constructed by the Michigan Aerospace Corporation, is designed after the highly successful triple etalon FPI instrument flown on the Upper Atmosphere Research Satellite. Presently, this observatory has been operating in campaign mode at Huancayo, Peru. An example of SOFDI results during a geomagnetic storm is presented in Figure 1, and perhaps the point of greatest interest quite unexpected is the large variability seen in the zonal neutral winds.

For 630-nm nighttime measurements of thermospheric winds and temperatures, a low-cost imaging FPI design approach using a fixed-gap etalon (1.5 cm) with diameters of 42 mm or 70 mm and coated with a reflectivity of 77-78% has been quite successful in obtaining high-quality thermospheric wind and temperature data. The

advantage of the fixed-gap imaging FPI design is that the spectral information is captured through a single exposure of a CCD, rather than having to scanning the instrument through either pressure or etalon-gap separation. The details of this type of design can be found in Shiokawa et al. (2012), which summarizes a typical instrument's characteristics. The FPI interference pattern is detected with a high-quality, low-noise CCD camera allowing for the long integration times (~5 min) required for analysis of the weak 630.0-nm emission. Dynamical real-time processing of each sky image allows for high-quality wind and temperature data to be collected varying the integration time while maintaining a constant signal to noise ratio.

The results in Figure 2, taken from Meriwether et al. (2013), illustrate the comparison of the monthly climatologies of thermospheric zonal winds obtained from two FPIs in northeastern Brazil with results from the Whole Atmosphere Model (see review by Akmaev, 2011). Such comparisons demonstrate the importance of continual FPI measurements, which can provide a reference against which the success of a model can be measured.

A more extensive FPI network is being developed in North America. Figure 3 shows an example of the latitudinal distribution of the neutral winds and how they change during a geomagnetic storm. The monthly mean of the thermospheric wind vectors (white arrows) provide a reference against which the strong equator-ward surge in neutral winds during the storm (red arrows) can be seen. The on-going science analysis of data from this FPI network will be helpful in improving our understanding of how these high latitude events ultimately have an impact upon the TI dynamical processes of the whole globe.



Building on the successes of the past several years operating small-scale networks of FPIs, long-range plans for the future envision the development of a continental-wide (or even global) distribution of FPI observatories. The aim would be the real-time internet transfer of the

FPI results to a central location where data assimilation into the current sophisticated grid-point physics-based model of the global thermospheric dynamics would enhance the accuracy achieved allowing for the successful predictions of atmospheric drag and enhanced modeling of space-weather phenomena.

Article 6

Concentric waves and short-period oscillations observed in the ionosphere after 2013 Moore EF5 tornado

M. Nishioka, T. Tsugawa, M. Kubota and M. Ishii

National Institute of information and Communications Technology, Tokyo, Japan



Michi Nishioka

Concentric wave structures and short-period oscillations were observed in dense wide-coverage TEC maps one to two hours after the massive tornado hit in Moore, Oklahoma, USA on May 20, 2013. Figures 1a-c show the TEC maps for 20:00, 21:00, and 22:00 UT, respectively. The TEC map at 20:00 UT shown in Figure 1a

does not exhibit any remarkable TEC variations. At 21:00 UT, as shown in Figure 1b, several circular wavefronts appeared, as indicated by the solid concentric circles whose center is designated by a cross. The wavefronts spread over North America as shown in Figure 1c. These concentric waves appeared to propagate for more than seven hours over North America.

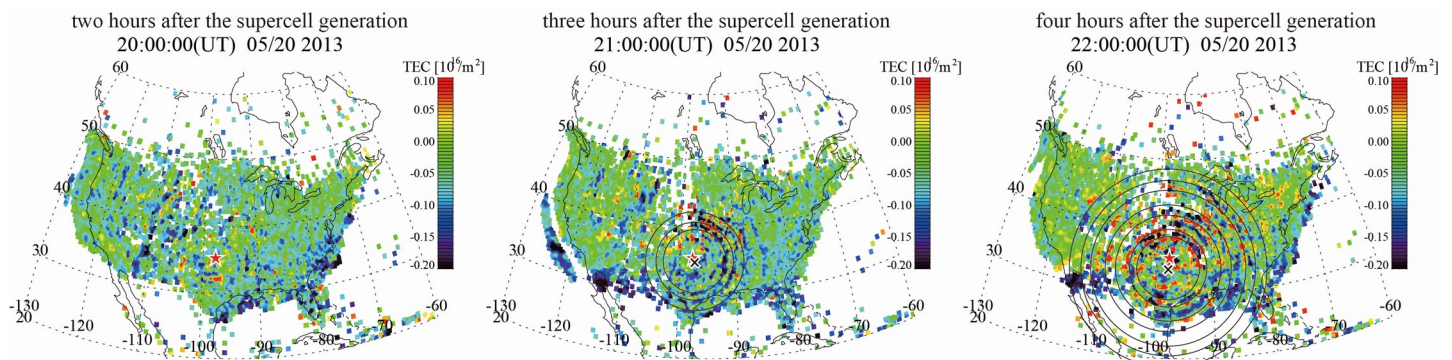


Figure 1. Concentric waves observed in TEC perturbation maps. TEC values were calculated from more than 2,600 ground based GPS receivers data in North America. The TEC perturbation values are derived by subtracting 20-minute running average from the TEC value. The city of Moore is represented by a red star. The circles represent the concentric wavefronts detected by the TEC map. The center of the concentric waves is designated by a cross mark.

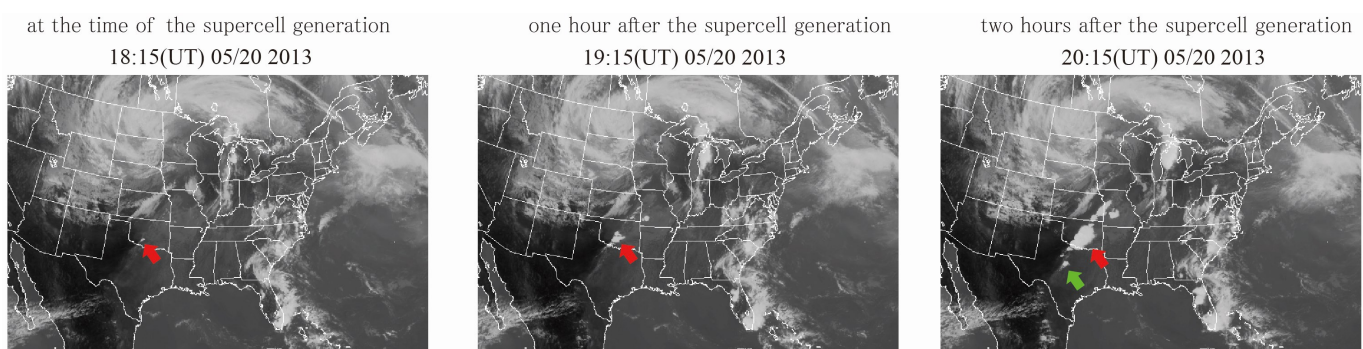


Figure 2. Supercells captured in Infrared images by the GOES-13 satellite. The brightness of the image represents cloud-top height. The red and green arrows indicate the location of the developing supercell in Oklahoma and Texas, respectively.

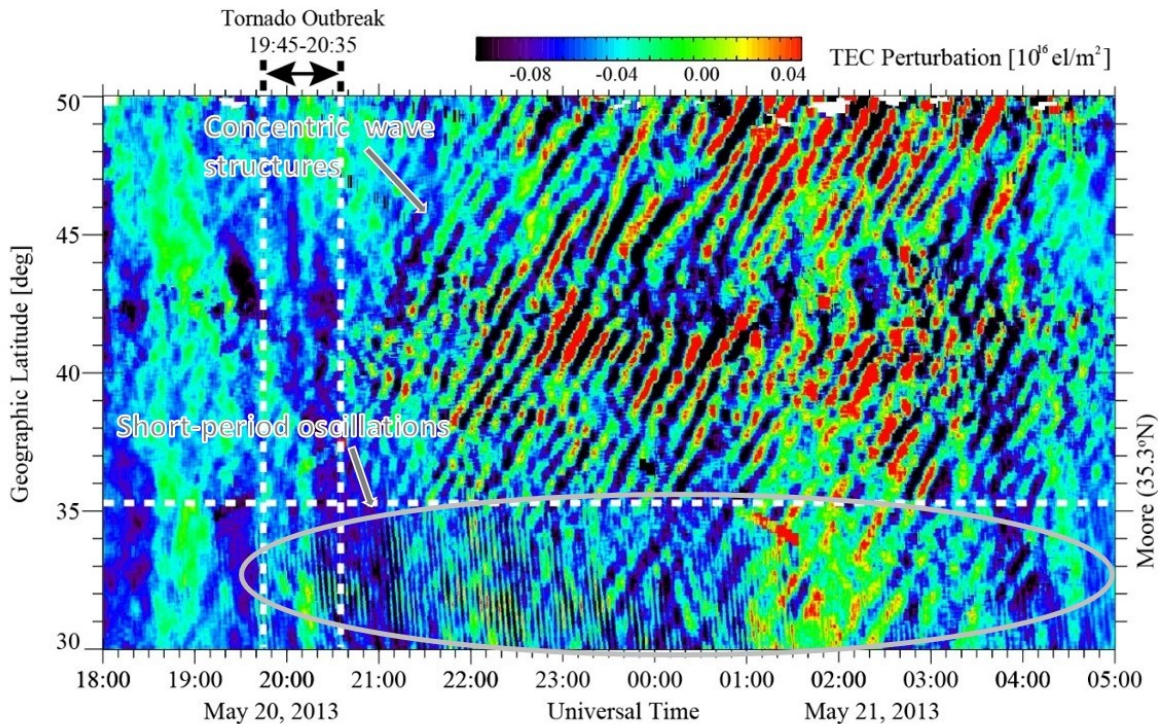


Figure 3. Time-latitude cross-section of Figure 1 at the longitude of Moore, 97.7°W, from 18:00 UT on 20 May to 05:00 UT on 21 May. The horizontal dashed line represents the location of Moore. The vertical dashed lines indicate the beginning and end of the tornado outbreak around Moore.

The center of the concentric waves shown in Figures 1b-c corresponds to the origin of a massive tornado outbreak on 20 May 2013. The tornado touched down at 19:45 UT and travelled through the city of Moore. It was ranked as an EF-5 tornado, which is the powerful one. The evolution of the supercell that produced the massive tornados was captured by a NOAA GOES satellite. Figures 2a-c show infrared images acquired from the GOES-13 satellite at 18:15, 19:15, and 20:15 UT, respectively. As indicated by red arrows in Figure 2a-c, a supercell began to appear at 18:15 UT and developed within a few hours. The EF-5 tornado touched down at approximately the same location at which the supercell developed. This location also corresponded to the center of the concentric waves in the ionosphere. Another supercell was generated at 20:15 UT at Texas, as indicated by a green arrow in Figure 2c.

A detailed analysis was conducted using the time-latitude cross-section of Figure 1 at 97.7°W, where the tornado touched down. Figure 3 shows the TEC perturbation components for geographic latitudes of 30° to 50°N from 18:00 UT on 20 May to 05:00 UT on 21 May 2013. In the region north of Moore (35.3°N), more than 20 wavefronts appeared to propagate northward, corresponding to the concentric waves shown in Figure

1. The period was about 15 minutes. The structures had a horizontal wavelength of approximately 100 km and a constant horizontal phase velocity of approximately 170 m/s. The waves reached 50° N latitude (1600 km north of Moore) after three hours.

In addition to the northward-propagating component of the concentric wave in the region north of Moore, a short-period TEC oscillation was observed at the south of Moore, between 30°N and 35°N latitudes. As shown in Figure 3, the oscillation began to appear at approximately 19:30 UT and continued till 05:00 UT on 21 May. The period was about four minutes. The oscillation lasted for about eight hours.

A comparison between the TEC maps and infrared cloud images from the GOES satellite indicates that the concentric waves and short-period oscillations are caused by supercell-induced atmospheric gravity waves and acoustic resonances, respectively. This observational result provides the first clear evidence of a severe meteorological event causing atmospheric waves propagating upward in the upper atmosphere and reaching the ionosphere. The details of this study is presented in Nishioka *et al.* [GRL, 2013].



Upcoming meetings related to CAWSES-II TG4

Conference	Date	Location	Contact Information
CAWSES-II2013 Symposium	Nov. 18-22, 2013	Nagoya, Japan	http://www.stelab.nagoya-u.ac.jp/cawses2013/ .

From the Editor

Michi Nishioka,
Editor of the CAWSES-II
TG4 newsletter

(nishioka_at_nict.go.jp)

National Institute of Information and
Communications Technology, Tokyo, Japan



It is my great pleasure to publish the CAWSES-II TG4 newsletter, issue 13. I hope all readers enjoyed this issue as well as the past issues. This issue is the final one of CAWSES-II TG4 newsletter. I believe the purpose of this newsletter, to make more communication among scientists related to the CAWSES-II TG4, is also achieved through the all issues of the newsletter.

I have been the editor of this newsletter for three and half years. It passed by like a flash, but when I look back at all issues, I am surprised how many researchers contributed articles to our newsletter. The number of the articles is 73. I really appreciate all authors who kindly provided their articles. The authors are from 23 countries; Australia, Brazil, Canada, Czech Republic, China, Côte d'Ivoire, German, India, Israel, Italy, Japan, Kazakhstan, Korea, Nigeria, Peru, Russia, Spain, Sweden, Switzerland, Taiwan, Thailand, United Kingdom, and United States of America. I really enjoyed communicating with the international authors through editing this newsletter. In addition, I got some message from readers after I published each issue, which made me happy. I am afraid that this would be the last chance for me to send messages through the newsletter, but I am looking forward to seeing all of you one day.

Regards,
Michi